Experimental research and finite element analysis of square concrete columns confined by FRP sheets under uniaxial compression

P. Feng, X. Z. Lu & L. P. Ye
Department of Civil Engineering, Tsinghua Univ., Beijing, China

ABSTRACT: In order to investigate the behavior of square concrete columns confined by fiber reinforced polymer (FRP) sheets, five specimens were tested and analyzed using finite element method (FEM). The loading behaviors of the confined concrete columns under uniaxial compression can be divided into three phases. As confirmed by experimental results, finite element analysis (FEA) can effectively simulate the behavior of square columns confined by FRP sheets when the proper numerical model is adopted. Based on the test and FEA, the stress distributions and the stress development are obtained. This provides theoretical understanding for establishing the stress-strain curve model. It is suggested that the FEM is a powerful method for further research on numerical test and parameter analysis.

1 INTRODUCTION

Repair and seismic retrofit of concrete structures with FRP (Fiber Reinforced Polymer) has become increasingly common in developed countries and China due to its high strength and light weight. There are many engineering applications in which FRP was bonded onto the surface of reinforced concrete elements to improve their strength and ductility. One of the most important applications is the confinement of concrete columns with FRP sheets. It is an effective method proved by many engineering applications and experiments (Mirmiran 1995, 1997).

In order to understand the behavior of confined concrete columns with wrapped FRP sheets and to predict the behaviors better, the mechanical mechanism needs to be studied. In 1982, Fardis et al. (1982) began this research, proposing a hyperbolic function for concrete cylinders wrapped with bi-directional FRP sheet under uniaxial loading. Nanni et al. (1995) further improved this model. Recently, many researchers, such as Samaan et al. (1998), Rochette et al. (1996), Komakatani et al. (1998), have proposed models for concrete cylinders and square columns strengthened with FRP sheets.

Most of models for square columns, however, are based on test curves and therefore cannot explain the mechanism. Most importantly, they cannot determine the distribution and the development of stresses for rectangular section. The finite element numerical simulation shows promise as a good method for studying this type of mechanism and has been applied widely in engineering and research. Rochette & Labossiere (1996) used an incremental finite element approach to study square columns. They modeled concrete as an elastic-perfectly plastic material, and adopted the Drucher-Prager failure criterion. Their FEA results compare favorably with their test results. In this paper, the finite element method is used to analyze the mechanism and the behavior with more rational model and failure criterion. Theoretical results are contrasted with test results. Based on the comparison, the stress distributions, as well as the stress development in concrete and in FRP sheets are obtained, which provides theoretical understanding for establishing a reliable stress-strain curve model.

2 EXPERIMENTAL METHOD

2.1 Specimens

Uniaxial compression test was carried out with five 200×200×600mm square specimens. In order to imitate the columns in an actual building, 4 longitudinal steel bars of 10mm diameter were settled in the corners in the columns and 3 steel hoops of 6mm diameter were placed at intervals of 200mm. Two additional hoops were used to reduce the intervals into 45mm at the end of the columns to prevent local damage. In order to prevent the fiber from being folded and to decrease the concentration of stress, the section corners were chamfered to a radius of 20mm.

Glass FRP (GFRP) sheets and carbon FRP (CFRP) sheets were used. Fibers fully wrapped

columns around the horizontal cross section. The properties of materials in columns are listed in Table 1. One of the specimens was not wrapped, which is a control. Table 2 shows all specimens.

Table 1. Properties of materials

Concrete	Cube strength f_{cu}(MPa)	Prism strength f_c(MPa)	Elastic modulus E_c(MPa)
	27.8	21.1	2.95×10^4
Bars	Bars' strength f_y (MPa)	Hoops' strength f_y (MPa)	Elastic modulus E_s (MPa)
	342.0	290.8	2.10×10^5
FRP sheets*	Thickness	Ultimate strength	Elastic modulus
	t (mm)	f_{FRP} (MPa)	E_{FRP} (MPa)
GFRP	0.304	900	6.5×10^4
CFRP	0.111	3550	2.35×10^5
Resin	Specials for fibers applied by manufacturers.		

* Manufacturers' data

Table 2. Outline of specimens

Specimen	Type	Number of plies	ρ_{FRP} (%)
C0	No wrap	None(To Control)	0
CM1(GC1)	GFRP	1 ply (Full wrap)	0.608
CM2(GC2)	GFRP	2 plies (Full wrap)	1.216
CM3(GC3)	GFRP	3 plies (Full wrap)	1.824
CM4(CC1)	CFRP	1 ply (Full wrap)	0.222

In tabel 2, ρ_{FRP} is the volume ratio of fibers to concrete, which is determined by

$$\rho_{FRP} = \frac{4nt}{D} \tag{1}$$

where n is number of FRP sheet layer, t is the fiber sheet's thickness of each layer, D is the side length of column section.

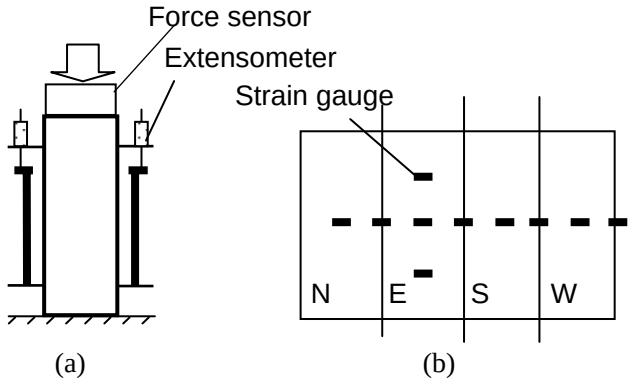

Figure 1a. Sketch of test
Figure 1b. Strain gauge on specimens' surface

A force sensor was placed on top of the specimen to measure the compression loads. Two extensometers, which are used to measure the axial deformation over a 400mm gauge length in the middle of the specimen, were symmetrically fixed at two sides of column. Ten strain gauges were pasted on the surface of fiber sheet for each specimen. Fig. 1 shows all measuring equipment used in the test.

2.2 Test

The load-displacement curves of all specimens were drawn in test and shown in figure 2. Compared with C0, it can be seen that the load-carrying capacity and the deformation capacity of the specimens wrapped with FRP were improved greatly.

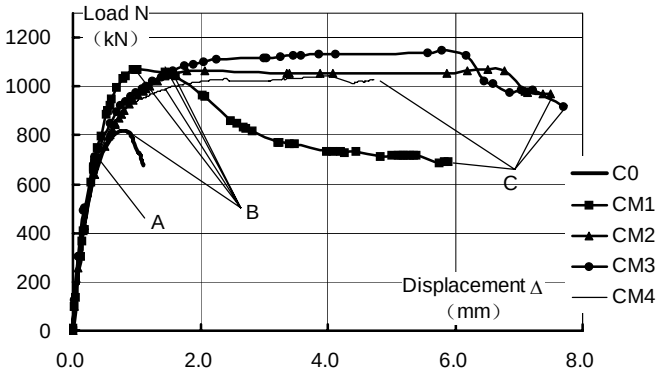

Figure 2. Experimental load-displacement curves

The loading behavior of the specimens wrapped with FRP can been divided into three phases. The first phase OA is from origin point O to A. Point A is corresponding to the load of $0.8N_p$ (N_p is the peak load of C0). In this phase, where all curves are almost the same, lateral expansions were very small, and the fiber stresses very low. The fiber stresses at point A are only about 5% of their strength. When the load exceeded $0.8N_p$, the fiber strain and stress began to increase. When the load reached about N_p, cracking noises was heard in specimens, which was the fiber being tensed. At this moment the steel bars had yielded. For FRP wrapped specimens, although the load rose slowly after N_p, the fiber strains rose rapidly. The loading curve of CM1 fell after reaching its peak, while the curves of the other specimens passed a turning point and continued nearly horizontal direction, the load holding stable and the deformation increasing constantly. Only the load of CM3 rose with a small slope. The course from point A to the peak point of CM1 and the turning points of the FRP wrapped specimens, which are marked as point B, is the second phase AB. From point B to the failure point C is defined as the third phase BC. After point B the specimens had deformed largely in the axial direction. Several furrows could be seen on the FRP sheets' surface. Finally, the fibers burst suddenly and the column collapsed. All specimens' damage pattern was that of the fracture of fiber.

In the test, the ultimate strain of GFRP was about $9000\mu\varepsilon$, the ultimate strain of CFRP was about $8000\mu\varepsilon$. The fiber fracture usually took place near the point of contact between the straight edge and the corner arc. The columns shorten noticeably.

These three phases represent three states of the confined column. In the phase OA the concrete has less expansion and fiber takes little constraining effect; in the phase AB the concrete began to have a

large expansion and the fiber begins to be tensed; in the phase BC the concrete goes into a flowing plastic state until the fiber breaks.

3 FINITE ELEMENT METHOD

3.1 Material properties

All of the specimens were simulated with ANSYS (version 5.6), which offers a series of very robust nonlinear capabilities for designs and analyses, and is famous for its using in engineering. The concrete adopted SOLID65 element in ANSYS. SOLID65 is used for the three-dimensional modeling of solids with or without reinforcing bars (rebars). The solid is capable of cracking in tension, crushing in compres-sion, creep nonlinearity and large deflection geome-trical nonlinearity. Here, the model without rein-forcing bars was used. The failure criterion of con-crete was the William-Warnke model with 5 para-meters. The uniaxial stress-strain relation was defined according to Guo's curve (Guo & Zhang, 1982). The peak strength f_c=21MPa，initial young's modulus E_c=30GPa, and the other parameters in the model were assigned according to the data in the test.

The reinforcing bar adopted LINK8 element. LINK8 is a spar that may be used in a variety of engineering applications. The three-dimensional spar element is a uniaxial tension-compression element with three degrees of freedom at each node. Plasticity, creep, swelling, stress stiffening, and large deflection capabilities are included. The bar was modeled as an elastic-perfectly plastic material, and the strength was defined according to the data in the test.

The fiber sheets adopted SHELL41 element. SHELL41 is a 3-D element having membrane (in-plane) stiffness but no bending (out-of-plane) stiffness. It is intended for shell structures where bending of the elements is of secondary importance. The fiber sheets were defined as an anisotropic material. The strength in the perpendicular direction was $1/10^6$ of that in the fiber direction. The FRP sheets were defined as an elastic material, which has been demonstrated in many tests. The ultimate strengths used the manufacturers' data. When the fiber's stress reaches the ultimate strength, the calculating stops.

3.2 Mesh and boundary condition

Figure 3 shows meshed column and boundary conditions. It is an assumption that all joints of elements satisfy displacement coordination, including the intersections of fiber, rebars and concrete. From the symmetry of column, a quarter was used in calculations. The end of column was fixed where there was no freedom degree. Uniform displacement compressive loading was adopted in the calculation.

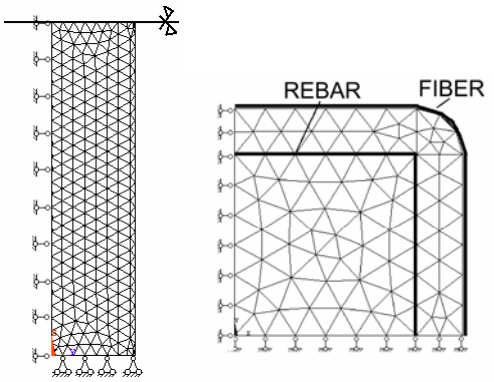

Figure 3. Meshed column model

4 COMPARISON

Favorable results were acquired by FEM. Figure 4 shows the comparison of stress-strain curves of the specimens obtained through the FEA calculation and test. Table 3 contrasts differences of maximum axial stresses in the columns, all of which are less than 10%. The maximum axial stresses by FEM are average stresses of whole sections. It was determined by the axial load divided by the section area. It can be seen that the two results are nearly identical.

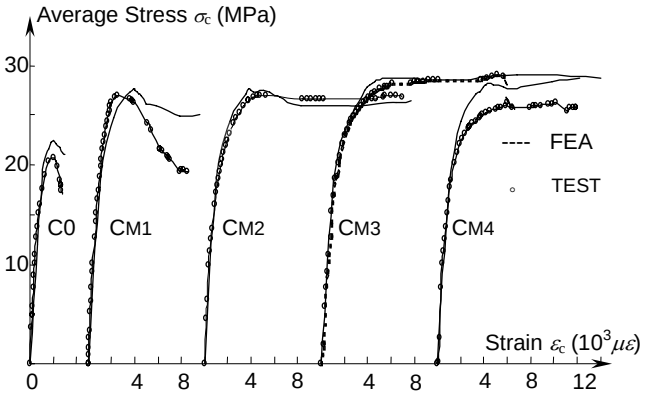

Figure 4. Comparing stress-strain curves

Table 3. Comparing maximum axial stresses

Specimen	C0	CM1	CM2	CM3	CM4
Test (MPa)	20.72	26.93	27.04	28.99	26.26
FEM (MPa)	22.43	27.67	27.72	28.60	28.22
Difference (%)	8.25	2.75	2.51	-1.96	7.46

Figure 5 shows the comparison of development curves of FRP sheets' strain between calculation and test. Following properties can be observed:

(a) The curves correlate favorably during the lower strains, ε_c <5000$\mu\varepsilon$, that is to say that, in the phase OA and phase AB the calculated curves are very close to the test ones. And some serrations and

strays occur in the lower strains phases because large strain exceeded range of strain gauges.

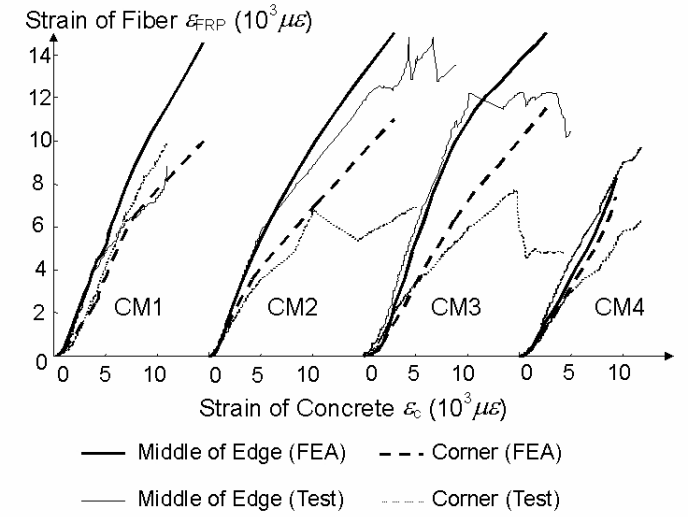

Figure 5. Strain developments of Concrete and FRP

(b) The strain curves of middle of edge correlate better than that at the corner. The fiber strain gradient in thickness direction causes it. The strain measured by the strain gauge is the strain at the outer surface of the sheet, while the calculated strain is an average value. This effect is more obvious on the corner fiber. This effect can explain why the calculated and test strain curves of CM1 are closer than those of CM2 as well as why those of CM2 closer than CM3, because the thicker the fiber, the less uniform the strain in the sheet.

According to the comparisons, it can be seen that the results of inelastic finite element numerical simulations with ANSYS under proper models have consistency with the test ones. Therefore, the calculated results can be used to analyze the mechanical mechanism of the specimens.

5 ANALYSIS OF STRAIN AND STRESS

The distributions of strain and stress in the specimens can explain their behavior in essence. The fiber strain and the concrete stress are taken for analysis below. Since the fiber is an elastic material, the distribution of fiber stress is similar to its strain.

5.1 Vertical distribution of strain in fibers

During the lower strain course, the vertical distribution of the fiber strain is nearly uniform. However, the stress near the middle of columns rises steeply when the axial load is close to ultimate value. Figure 6 shows the distributions in the vertical direction of calculated fiber stress ratios at the moment of fiber break.

The stress in the column ends is very small due to less expansion of the fixed ends in the model, while a stress peak appears at mid-section. It has been demonstrated by the test that the fiber fails firstly in the middle of columns. It shows that outer constraint can reduce the fiber's confining stress. Thus the most effective improvement should be to add a fiber sheet loop in the middle of the columns.

With multiplication of the fiber sheet, the constraint to the column is enhanced. The stress tends to be uniform, and the confined volume of concrete in high stress increases. Thus the column with more fiber has a larger ruined zone in final. This can be seen clearly by contrasting the damaged specimens.

CM4 was wrapped with CFRP sheet that has a higher elastic modulus than GFRP. Hence, the constraint is more effective and the stress distribution is more uniform.

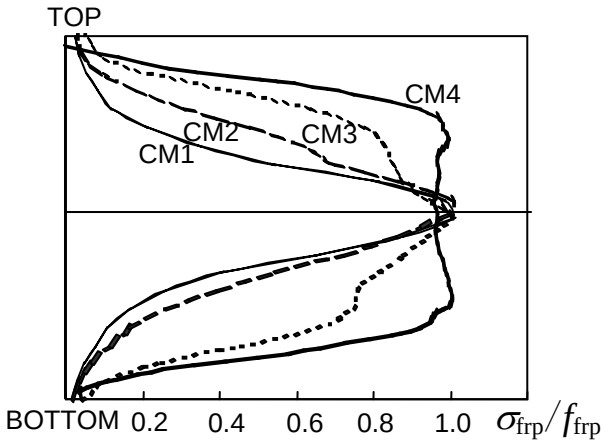

Figure 6. Vertical distributions of calculated stress ratio

5.2 Circumferential distribution of strain in fibers

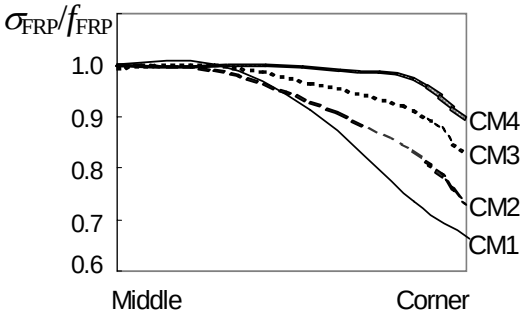

Figure 7. Circumferential distributions of calculated stress ratio

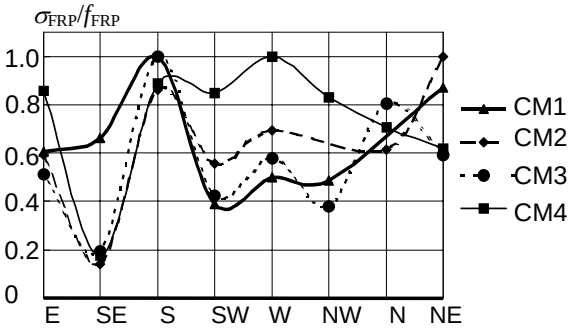

Figure 8. Circumferential distributions of tested stress ratio

During the lower strain course, the circumferential distribution of fiber strain is nearly uniform also. When approaching the breaking load, the fiber stress in the section away from the middle is still uniform. However, near the middle section the tensile stress of fiber has an obvious difference in the circumference. Figure 7, represented in a half edge of the column, shows the circumferential distributions of calculated fiber stress ratios at the moment of fiber break. And Figure 8, represented in the four unwrapped faces of columns, is the tested stress ratios before the strain gauge failure.

It can be seen that stresses at the corner are less than that at the middle of the edge. At the midpoint of side there is little constraint to resist the expansion of concrete due to the small bending stiffness of FRP sheet. Larger deformation at this point results in higher stress of the fiber. Test and calculation both proved it. However, the breaking point is never located in middle of the side in the test. It argues that the stress concentration at the point of contact is the immediate cause for fiber break.

5.3 Distribution of concrete stress at column section plane

Figures 9 to 11 show the calculated concrete stress distributions in the middle section. Every square is a top right quarter section of the column. The light color means a large value of stress and the deep color means small stress.

Figure 9 shows the concrete stress distributions of CM3 at the axial load 1136kN. The left is the axial compressing stress and the right is the lateral confining stress. At this stage the specimen is just turning into the third phase. The average axial stress is 28.4MPa, and the strain is 4656$\mu\varepsilon$.

Figure 10 shows the concrete stress distributions of CM1 at axial load 1100kN. At this point the specimen is on the peak and is turning into the third phase. The average axial stress is 27.5MPa, and the strain is 4050$\mu\varepsilon$.

Figure 11 shows the concrete axial stress distributions of CM3. The left shows the turning point under a load of 1136kN and the column's strain is 4656$\mu\varepsilon$, the right shows the breaking point with a strain of 25500$\mu\varepsilon$.

From these figures some behavior characteristics can be seen. The strongest constraint zone is at the corner of column section and drops gradually along the diagonal. On both sides of diagonal the constraint becomes less, and the weakest constraint appears at the middle of the edges. Thus a X-shaped stress ridge occurs under the compression load. It is very similar to the square concrete column confined by steel hoops.

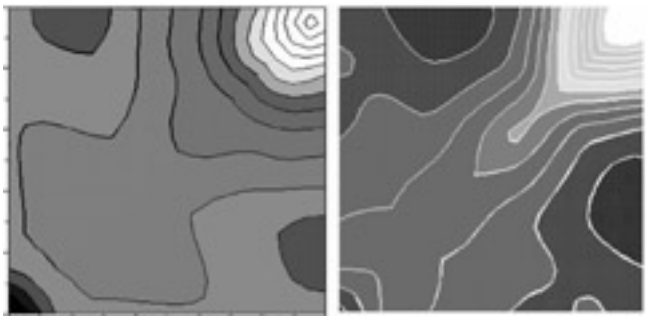

Figure 9. Concrete stress distributions of CM3

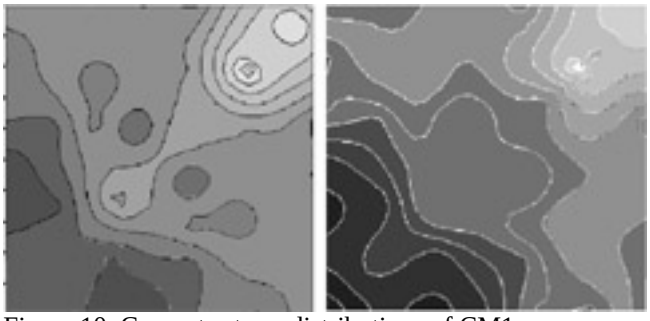

Figure 10. Concrete stress distributions of CM1

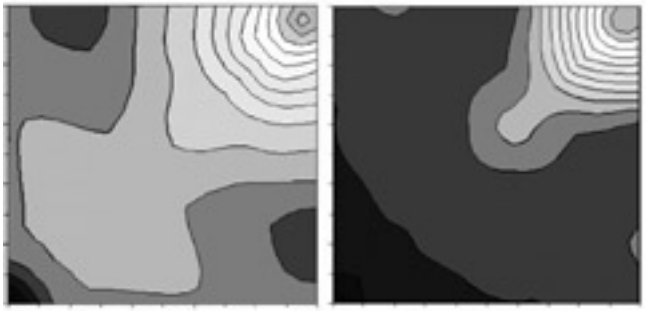

Figure 11. Concrete axial stresses of CM3 at turning point and breaking point

The amount of FRP sheets affected the stress distribution, but only on distribution at the corner and obviously at the turning point. The largest axial stress in CM1 section is 30MPa at the corner, which can be increased to 40MPa in CM3 for tri-layer FRP sheets. Meanwhile, the axial stress at the middle of edge in CM1 is about 26MPa, that is the same as in CM3. Because the corner with a strong constraint is only a fraction of whole section (about 20% area for 20mm corner radius of 200mm side length), the carrying capacity cannot be enhanced more. For instance the maximum loads are 1070kN for CM1, 1100kN for CM2, 1148kN for CM3.

Comparing turning point and breaking point, the stress concentrates at the corner more obviously. The higher the stress at the corner, the steeper the gradient becomes. At the breaking point, the ultimate state of the columns, there are four sharp stress peaks at the corners and a plain in the center.

6 CONCLUSIONS

The behavior of square concrete columns confined with FRP sheets was studied by the testing and FEA

outlined in this paper. The following conclusions were obtained:

1 FEM is an effective method for analyzing the behavior of concrete elements strengthened with wrapped FRP sheets. ANSYS with a great variety of element models can be used.
2 The behavior of the square concrete columns confined by FRP sheets under uniaxial compression can be divided three phases. Each phase means a stress state of columns. The stress-strain curve model will be built according to these three phases.
3 The area with strong constraint at the corners and the average stress in the central plain determine the carrying capacity of square columns confined by FRP sheets. It is a graphic explanation for the behavior of columns, and provides theoretical understanding for establishing the model.
4 The radius of the corner in square columns affected the behavior in two ways. It determines the area in strong constraint and stress concentration effect. The larger radius can expand the strong constraint zone and diminish the stress concentration.

REFERENCE

Fardis, M. N. & Khalili, H. 1982. FRP-encased concrete as a structural material. *Magazine of Concrete Research* 34(121): 191-202.

Guo, Z. H. & Zhang, X. Q. 1982. Experimental study on concrete stress-strain curve. J*ournal of Building Structure* 3(1): 1-12. (In Chinese)

Komakatani, G., Kawashima, I. & Noshikwma, J. 1998. Model stress-strain curve of concrete columns confined by carbon FRP sheet, *Civil institute, Symposia, Japan* 592(39):37-52.(In Japanese)

Mirmiran, A. 1995. Concrete composite construction for durability and strength. In IABS-EAIPC-IVBH (ed.), *International association for bridge and structural engineering symposium report. San Francisco, 1995.* Zurich: Honggerberg.

Mirmiran, A. & Shahaway, M. 1997. Behavior of concrete columns confined by fiber composites. *Journal of Structural Engineering* 123(5): 583-590.

Nanni, A. & Bradford, N. M. 1995. FRP jacketed concrete under uniaxial compression. *Construction & Building Material* 9(2): 115-124.

Rochette, P. & Labossiere, P. 1996. A plasticity approach for concrete columns confined with composite materials, In M. M. El-Badry (ed.), *Advanced composite materials in bridges and structures; Canadian Society for Civil Engineering, Montreal, 1996*: 359-366.

Samaan, M., Mirmiran, A. & Shahawy, M. 1998. Model of concrete confined by fiber composites. *Journal of Structural Engineering* 124(9): 1025-1031.